Preparation, Characterization, and Complete Heteronuclear NMR Resonance Assignments of the Glutaredoxin (C14S)−Ribonucleotide Reductase B1 737−761 (C754S) Mixed Disulfide[†]

Marcelo J. Berardi, Cynthia L. Pendred, and John H. Bushweller*

Department of Chemistry, Dartmouth College, Hanover, New Hampshire 03755

Received December 1, 1997; Revised Manuscript Received February 25, 1998

ABSTRACT: The first committed step in de novo DNA biosynthesis involves the conversion of ribonucleotides to the corresponding deoxyribonucleotides catalyzed by the enzyme ribonucleotide reductase. Reduction of disulfides in ribonucleotide reductase is essential and is catalyzed by the protein disulfide reductants glutaredoxin or thioredoxin. The interaction region between *Escherichia coli* glutaredoxin-1 and *E. coli* ribonucleotide reductase has been localized to the C-terminal end of the B1 subunit of ribonucleotide reductase. We have demonstrated that a 25-residue peptide corresponding to this C-terminal sequence is a very good substrate for glutaredoxin via a fluorescence assay and that this peptide binds in a specific manner via isothermal titration calorimetric measurements. By selectively mutating the two cysteines in the peptide, we have identified the electrophilic cysteine as C759 (B1 numbering) and prepared a mixed disulfide between *E. coli* glutaredoxin-1 (C14 → S) and the C759 monothiol form of the peptide. The peptide and the protein have been labeled with ^{13}C and ^{15}N, and complete heteronuclear NMR resonance assignments have been completed for both the peptide and the protein in the complex. By using half-filtered NOESY spectra, intermolecular NOEs between the protein and the peptide have been identified and the binding site on glutaredoxin has been mapped. The electrostatic charge distribution of the protein in this region is very positive, thus providing an excellent match for the highly negatively charged peptide. In addition, the electrostatic potential of the peptide provides a rationale for the observed cysteine selectivity in the reaction between glutaredoxin and the B1 peptide.

Glutaredoxins are a family of proteins involved in electron-transfer reactions via the reversible oxidation of two active-site thiols to a disulfide bond. Glutaredoxins have been identified in numerous species, including *Escherichia coli*, bacteriophage T4, vaccinia virus, yeast, rabbits, pigs, and humans (*1*−*9*). Additionally, a total of three glutaredoxins have now been identified in *E. coli* alone (*10*). Glutaredoxins have been shown to be essential for the glutathione (GSH[1])-dependent reduction of ribonucleotides to deoxyribonucleotides by ribonucleotide reductase (*11*−*14*). Glutaredoxins have also been shown to play a role in the reduction of sulfate (*15, 16*), arsenate (*17, 18*), and ascorbate (*1, 19*). Glutaredoxins preferentially reduce GSH-containing mixed disulfides (*19, 20*), because of the GSH binding site present on the protein (*21*), but can also function as general protein disulfide reductants. This preference for GSH-containing mixed disulfides implies that glutaredoxins are also likely to have a role in glutathionylation and deglutathionylation of proteins, an important element of the cellular response to oxidative stress (*22, 23*).

Glutaredoxins are part of a superfamily of proteins including thioredoxin, DsbA, GSH transferases, GSH peroxidases, and glutaredoxin which all share a common fold (*24*). Glutaredoxins are distinguished from the related protein disulfide reductants termed thioredoxins by their differential reactivity. Glutaredoxins are reduced by GSH but not by thioredoxin reductase, whereas thioredoxins are reduced by the corresponding thioredoxin reductase but not by GSH. As mentioned above, glutaredoxins preferentially catalyze GSH mixed disulfide oxidoreduction reactions, whereas thioredoxin acts as a quite general protein disulfide reductant. In *E. coli*, both thioredoxin and glutaredoxin can function as effective protein disulfide reductants for ribonucleotide reductase. However, mutants deficient in glutaredoxin (*25*) and the 10-fold lower K_m of Grx for ribonucleotide reductase suggest that Grx may be the dominant in vivo reductant for ribonucleotide reductase. Site-directed mutagenesis of the five thiols of the B1 subunit of *E. coli* ribonucleotide reductase has shown that Cys 439 is the protein radical that abstracts the 3′ proton, whereas the remaining four cysteines form two redox-active dithiol−disulfide pairs (*26, 27*). Cysteines 225 and 462 were identified as the active-site reductant for the radical cation intermediate, whereas cysteines 754 and 759, located at the C-terminal end of the B1 subunit, were shown to be the

[†] These studies were supported by funds provided by Dartmouth College.

* To whom correspondence should be addressed.

[1] Abbreviations: DTT, dithiothreitol; Grx, *E. coli* glutaredoxin-1; GrxC14S, *E. coli* glutaredoxin-1 with Cys 14 → Ser; GSH, glutathione; GSSG, oxidized form of glutathione; HED, β-hydroxyethylene disulfide; HPLC, high-performance liquid chromatography; IEF, isoelectric focusing; IPTG, isopropyl β-D-thiogalactopyranoside; NMR, nuclear magnetic resonance; NOE, nuclear Overhauser effect; OD_{600}, optical density at 600 nm; TFA, trifluoroacetic acid.

S0006-2960(97)02924-3 CCC: $15.00
Published on Web 04/07/1998

interaction site for glutaredoxin and thioredoxin (*28, 29*). Indeed, a Cys 439 → Ser mutant of B1 was demonstrated to have protein disulfide reductant activity but no detectable ribonucleotide reduction (*30*). The recent solution of the X-ray crystal structure of the B1 subunit of *E. coli* ribonucleotide reductase (*31*) has confirmed the active site location of cysteine 439 and the proximity of cysteines 225 and 462. Interestingly, the 24 C-terminal amino acids were not observed in the crystal structure, potentially indicating a high degree of mobility for this region of the polypeptide. Thus, there is no structural information regarding the site of interaction with glutaredoxin and thioredoxin.

The NMR solution structures of several mixed disulfide intermediates with mutated forms of the protein disulfide reductant have recently been reported, including a mixed disulfide between *E. coli* glutaredoxin and glutathione (*21*) as well as mixed disulfides between human thioredoxin and peptides derived from NFκB and Ref-1 (*32, 33*). These structures have elicited the basis for recognition in these related proteins. Here we report analysis of ribonucleotide reductase B1 C-terminal peptides as substrates for glutaredoxin as well as measurement of binding affinity via calorimetry and the preparation of a mixed disulfide between *E. coli* glutaredoxin-1 (C14S) and *E. coli* ribonucleotide reductase B1 736−761 (C754S). In addition to conventional biochemical characterization of the mixed disulfide, we have obtained the complete heteronuclear NMR resonance assignments for the complex which provides confirmation of mixed disulfide formation and provides a map of the binding site for the peptide on glutaredoxin.

EXPERIMENTAL PROCEDURES

Protein Purification. The expression and purification of wild type *E. coli* glutaredoxin (wt Grx) as well as the mutant glutaredoxin Cys 14 → Ser (GrxC14S) have been previously described (*22, 34*). A total of 240 mg of GrxC14S and 50 mg of wt Grx were obtained from 4 and 1 L, respectively, of unlabeled TB media (Sigma). The uniformly ^{15}N-labeled GrxC14S was purified from 500 mL of [^{15}N]Celtone media (Martek Co.) with a yield of 25 mg. The ^{13}C, ^{15}N doubly labeled GrxC14S was purified from 250 mL of CN-Celtone (Martek Co.), yielding 16 mg after purification.

Optimal Peptide Length and Identification Of the Electrophilic Cysteine. The 15- and 25-mer peptides of wt (Cys 754 and Cys 759) and 15-mer single mutant (Cys 754 → Ser or Cys 759 → Ser) peptides were prepared by solid-phase synthesis (W. M. Keck Foundation Biotechnology Research Laboratory, Yale University, New Haven, CT). To remove the acetamidomethyl (Acm) protecting groups from the Cys residues of the wt peptides with concomitant formation of an intramolecular disulfide bridge between Cys 754 and Cys 759, a 4 mM peptide solution in acetic acid/water (8:1) was oxidized with a 5-fold molar excess of I_2 at 4 °C and purified by HPLC using a Vydac protein and peptide C18 column (mobile phase of 0.1% TFA/5% 2-propanol in H_2O with a linear gradient of 0 to 85% of 0.1% TFA/5% 2-propanol over the course of 50 min). To prepare the peptide−mercaptoethanol mixed disulfides, the crude peptides were first HPLC purified and lyophilized. A solution of 0.5 mM mutant peptide in 50 mM Tris (pH 7.0) was reduced with a 6-fold molar excess of DTT for 10 min at room temperature, then treated with a 20-fold molar excess of hydroxyethyl disulfide (HED) for 3 h at 4 °C, and finally purified by HPLC. Oxidized and mixed disulfide forms were confirmed by mass spectrometry (W. M. Keck Foundation Biotechnology Research Laboratory).

Fluorescence Assays. The reaction of 1.0 μM reduced are desalted wt Grx with 4.0 μM oxidized disulfide peptides and of 1.0 μM reduced and desalted wt Grx with 1.2 μM mixed disulfide mutant peptides in 50 mM Tris (pH 7.5) and 2 mM EDTA was monitored by the fluorescence intensity of Tyr 13 at 310 nm with excitation at 280 nm using a Shimadzu RF-1501 spectrofluorophosphometer, for a period of at least 100 s with a time resolution of 0.1 s.

Cloning, Purification, and Labeling of the 25-mer C-Terminal RR Peptide. The cloning and purification protocol is an adaptation of one previously described by Walsh and co-workers (*35*). For the construction of the fusion protein, two 78-mer DNA oligonucleotides were synthesized by Operon Technologies, Inc., each corresponding to the sense and antisense sequences of the peptide: 25 codons, 75 internally complementary base pairs, and an additional terminal overhang used for ligation into the *Alw*NI restriction site of the plasmid pET-31b(+) (Novagen). The annealed oligo was ligated with *Alw*NI-digested plasmid at 16 °C for 12 h using 10 units of T4 ligase/mL (50 mL total reaction volume). The plasmid DNA was extracted from the transformed cells using the QIAGEN plasmid purification kit, tested by restriction analysis, sequenced, and finally transformed into *E. coli* BL21pLyS cells for protein expression. Using this procedure, tandem repeats with an *n* of 1−3 were obtained. Transformed cells were incubated at 37 °C in LB media, using 100 μg/L carbenicillin and 50 μg/L chloramphenicol, and then diluted 1:100 into fresh media at an OD_{600} of 0.2. The culture was induced with 0.8 mM isopropyl β-D-thiogalactopyranoside (IPTG) at an OD_{600} of 0.6 and harvested after 8 h. The cells were resuspended in 50 mM Tris (pH 7.0) and lysed with four passes at 18 000 psi in a French Pressure Cell. For the construct with an *n* of 1, the KSI−peptide fusion remains in the pellet fraction as confirmed by SDS−PAGE analysis. The pellet was dissolved in a buffer of 50 mM Tris (pH 7.5), 500 mM NaCl, and 5 mM imidazole containing 6 M guanidine-HCl (binding buffer) and loaded onto a 10 mL His-Bind column. The protein was eluted using the same binding buffer with an imidazole concentration of 500 mM. Fractions of 3 mL were collected and analyzed by gel electrophoresis. Protein-containing fractions were collected and dialyzed overnight against two changes of 1 L of H_2O. A heavy white precipitate corresponding to the insoluble fusion protein was obtained. This was dissolved in 85% formic acid and digested with 3.0 g of CNBr, under N_2, for 22 h at room temperature. The remaining reaction was evaporated at 25 °C under vacuum and extracted three times with 15 mL of potassium phosphate (pH 7.5) and 250 mM NaCl, under N_2 for 6 h each time. To disrupt any mixed disulfides that might be formed, the extraction was titrated with DTT until an excess of reduced DTT was detected by HPLC after a 1 h reaction at room temperature, and then an additional 2-fold molar excess of DTT was added. The low molecular mass components were removed by size exclusion chomatography using a 50 mL BioRad P2 column and eluted with 25 mM Tris (pH 7.0) and 75 mM NaCl at 0.8 mL/min. Fractions

of 2 mL were collected and analyzed by HPLC using a Vydac protein and peptide C18 column (mobile phase of H_2O, 0.1% TFA, and acetonitrile, with 0.1% TFA from 0 to 85% over the course of 50 min). The pH of the fractions containing the peptide was adjusted to 9.0 with NaOH for 20 min at room temperature and then to 7.0 for 2 h. A C-terminal digestion of the resulting homoserine residue was performed with carboxypeptidase Y at a concentration of 0.5 unit/mL (sequencing grade, Boehringer-Mannheim) on a 0.1 mM peptide sample at 16 °C. Under these conditions, the reaction profile monitored by HPLC showed a new peak at 23.28 min that reached a maximum area after reaction for 80 min. A third peak is seen to build up with extended reaction times at 21.33 min. The reaction was stopped at different times with TFA at a final concentration of 0.1% and the mixture frozen at −80 °C. Fractions at 23.28 and 21.33 min were immediately frozen and lyophilized. Both fractions were active in our fluorescence assay. The mass spectrum of the peak at 23.28 min shows a predominant molecular species with a molecular mass of 2598.5 Da that compares well with the calculated molecular mass of 2598.0 Da for MH^+ of the oxidized 25-mer peptide. Uniformly ^{15}N-labeled peptide was purified from 1 L of M9 minimal media (*36*), 10 g/L glucose, and 1 g/L $(^{15}NH_4)_2SO_4$ as the sole source of nitrogen. When the culture reached an OD_{600} of 1.0, the cells were centrifuged at 15 °C and then resuspended in fresh media at 37 °C for 30 min and induced with 0.8 mM IPTG for 12 h at 37 °C, yielding 2.7 mg after purification. CN-Martek 9 medium was used for ^{13}C and ^{15}N labeling of the peptide with a yield of 2 mg/L.

Preparation of the Mixed Disulfide GrxC14S−B1 (736−761) (C754S) Complex. A 0.2 mM solution of the protein was fully reduced with a 10-fold molar excess of DTT for 30 min at room temperature. The DTT was removed and the buffer exchanged to 50 mM potassium phosphate (pH 7.5). The resulting DTT-free protein was treated with oxidized peptide at a peptide:protein ratio of 1.3:1. The excess peptide was removed by size exclusion chromatography on a Sephacryl S100 (Pharmacia) column, eluting with 50 mM potassium phosphate (pH 6.5) at 0.8 mL/min. The mixed disulfides were concentrated to 600 μL, yielding 1.1, 1.4, 1.8, and 1.0 mM samples of [^{15}N]Grx−B1, Grx−[^{15}N]-B1, [^{15}N,^{13}C]Grx−B1, and Grx−[^{15}N,^{13}C]B1, respectively. Concentrations of the protein and mixed disulfides were calculated using the extinction coefficient of Grx (*34*). Peptide concentrations were calculated by integration of HPLC peaks using as a reference a 25-mer sample which had its concentration determined by amino acid analysis. (W. M. Keck Foundation Biotechnology Research Laboratory).

Characterization of the Complex. The purity and stability of the mixed disulfide were evaluated by IEF gel electrophoresis and HPLC. The analysis of the purified complex shows a single species corresponding to the mixed disulfide by both methods. Two peaks with HPLC retention times corresponding to GrxC14S and reduced peptide standards were formed only when a sample of the purified mixed disulfide was reduced with a 10-fold molar excess DTT for 30 min at room temperature.

Isothermal Titration Calorimetry. The equilibrium constant for the formation of a mixed disulfide between GrxC14S and ribonucleotide reductase B1 (737−761) was determined by isothermal titration calorimetry (ITC). All experiments were performed at 25 °C on a Micro Calorimetry System MCS ITC (MicroCal Inc.). A 0.5 mM GrxC14S sample was treated with a 10-fold molar excess of DTT at room temperature for 25 min. Excess DTT was removed and the buffer exchanged by size exclusion chomatography using a 50 mL BioRad P2 column eluting with 50 mM potassium phosphate (pH 7.0) and 75 mM NaCl at 0.8 mL/min. A 0.15 mM GrxC14S solution was titrated with 1.0 mM oxidized 25-mer peptide. Ligand dilution enthalpies were subtracted from the titration, and data were fitted to a one-site model using Origin (MicroCal Inc.). Values were also measured for HED and GSSG under the same concentrations and conditions.

NMR Spectroscopy and Data Analysis. All NMR samples were dissolved in 50 mM potassium phosphate (pH 6.0), 0.1% NaN_3, and 5% D_2O. All measurements were carried out at 20 °C on a Varian UNITYplus 500 MHz NMR spectrometer equipped with a Nalorac actively shielded gradient triple-resonance probe and pulsed field gradients. In all these experiments, no sample spinning was used. Carrier frequencies were typically located at 4.72 ppm for ^1H, 117 ppm for ^{15}N, 45 ppm for aliphatic ^{13}C, 58 ppm for $^{13}C\alpha$, and 177 ppm for $^{13}C'$. NMR data were processed using the program PROSA 3.7 (*37*). Zero-filling was applied to all the indirect dimensions. Visualization and analysis of all the spectral data was carried out using the program XEASY (*38*). The experiments employed for the complete assignment of the complex are summarized in Table 1. Backbone and side chain assignments for the protein were completed from the information recorded from the [^{15}N,^{13}C]-Grx−B1 sample. Complete peptide assignments were obtained from recordings of the same experiments on the Grx−[^{15}N,^{13}C]B1 sample.

Electrostatic Potential and Dipole Moment Calculations. All calculations were performed using the commercial software package QUANTA96 (Molecular Simulations). Atomic radii and charges were obtained from the CHARMm 22 parameter file with a dielectric constant of 4 at 300 K. The lowest-target function NMR solution structure of the reduced form of Grx (*39*) was used in the electrostatic potential calculations. The Hγ of Cys 11 was removed, and the Sγ parameters of this cysteine were manually modified to represent a thiolate anion (S^-). All remaining residues were assumed to be in their usual protonation state at pH 7. The electrostatic potential was mapped on a solid surface defined by a 2.0 Å probe. The electrostatic distribution was represented with shades of blue for positively charged regions of potential energy from 0 to 20 kcal and shades of red for negatively charged regions with energies between 0 and −20 kcal. Color codes for values of greater than 20 or less than −20 kcal are blue and red, respectively.

The molecular dipole moment was calculated at 0.5 ps intervals in a trajectory of a 100 ps molecular dynamics simulation with a time step of 0.05 ps. The *x*, *y*, and *z* components as well as its magnitude did not change significantly during the simulation, yielding an average value of 260 D.

RESULTS AND DISCUSSION

Characterization of the Interaction of Glutaredoxin-1 with Peptides Derived from the C Terminus of E. coli Ribonucle-

Table 1: NMR Experiments Used for the Complete Assignment of the Mixed Disulfide Complex

sample	spectrum recorded	size	reference
[^{15}N]Grx−B1	2D ^{15}N−^{1}H HSQC	128 × 1024	*54*
	2D [^{15}N, ^{1}H]-hf-COSY	128 × 1024	*50*
	2D ^{15}N-hf-[^{1}H, ^{1}H]TOCSY (mixing times of 32, 56, and 80 ms)	32 × 128 × 512	*55*
	2D ^{15}N-edited hf-[^{1}H, ^{1}H]NOESY (mixing times of 120 and 200 ms)	32 × 128 × 512	*55*
	2D ^{15}N-edited hf-[^{1}H, ^{1}H]ROESY (mixing times of 80, and 120 ms)	32 × 128 × 512	*56*
	3D ^{15}N-edited hf-[^{1}H, ^{1}H]NOESY (mixing times of 120 ms)	32 × 128 × 512	*55*
[^{15}N,^{13}C]Grx−B1	3D HNCACB	32 × 36 × 512	*57*
	3D HN(CO)CACB	32 × 36 × 512	*57*
	3D CC(CO)-NH-TOCSY	20 × 64 × 512	*58*
	3D HCC(CO)-NH-TOCSY	22 × 64 × 512	*58*
	3D HCCH-TOCSY (mixing times of 8 and 16 ms)	32 × 96 × 512	*59*
	2D [^{13}C, ^{1}H]CT-HSQC aromatic	128 × 1024	*60*
	2D (Hβ)Cβ(CγCδ)Hδ aromatic	32 × 512	*61*
Grx−[^{15}N]B1	2D ^{15}N−^{1}H HSQC	128 × 1024	*54*
	3D ^{15}N-edited hf-[^{1}H, ^{1}H]TOCSY (mixing times of 30, and 56 ms)	32 × 64 × 512	*50*
	3D ^{15}N-edited hf-[^{1}H, ^{1}H]NOESY (mixing times of 120 ms)	32 × 48 × 512	*50*
Grx−[^{15}N,^{13}C]B1	3D HNCACB	32 × 36 × 512	*57*
	3D C(CC-TOCSY)-NNH	24 × 96 × 512	*58*
	3D HCCH-TOCSY (mixing times of 8 and 16 ms)	28 × 96 × 512	*54*

otide Reductase Subunit B1. Previous studies have demonstrated no effect of the presence or absence of GSH on the reduction of *E. coli* ribonucleotide reductase by *E. coli* Grx, suggesting that the C-terminal disulfide region of ribonucleotide reductase B1 is itself a good substrate for reduction by glutaredoxin (*40*), i.e., that there is a binding interaction between glutaredoxin and this region of B1. To verify experimentally that this C-terminal disulfide portion of B1 is in fact a good substrate, we have tested the reactivity of two peptides derived from the C terminus of B1. The X-ray crystal structure of the B1 subunit of *E. coli* ribonucleotide reductase shows no electron density for the 24 C-terminal residues; thus, there is no structural information for this region of the protein which is important for the interaction with thioredoxin and glutaredoxin (*31*). Therefore, we have prepared a peptide corresponding to the last 25 residues of B1 as well as a shortened 15-residue peptide to assess the importance of residues more distant from the disulfide on the reactivity. Previous work has shown that the fluorescence of the tyrosine in the active site of glutaredoxin shows a dramatic quenching upon going from the reduced to the oxidized form of the protein (*41*). We have employed this fluorescence method to assay the reactivity of our 15- and 25-mer peptides. Figure 1A shows the fluorescence data obtained upon treatment of reduced Grx with the oxidized form of glutathione, hydroxyethyl disulfide (HED), and the two peptides derived from the B1 subunit of ribonucleotide reductase. Glutathione is known to be a very good substrate for Grx due to the presence of a glutathione binding site on the protein (*21*), whereas hydroxyethyl disulfide is a poor disulfide substrate.

As expected, oxidized glutathione causes a very rapid oxidation of Grx that occurs during the time period of the mixing of the reactants, whereas HED displays a relatively slow rate consistent with its lack of binding interactions with

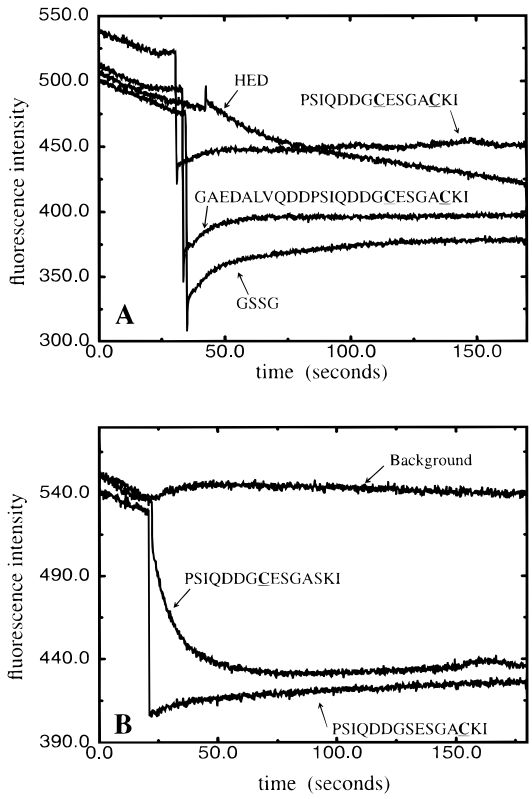

FIGURE 1: Assay of reactivity of glutaredoxin with various substrates monitored by tyrosine fluorescence at 310 nm (excitation at 280 nm). (A) Reactivity of Grx with β-hydroxyethylene disulfide (HED), the oxidized form of glutathione (GSSG), and oxidized 15- and 25-mer peptides corresponding to the C terminus of *E. coli* ribonucleotide reductase. (B) Reactivity of Grx with 15-mer C-terminal *E. coli* ribonucleotide reductase peptides with one cysteine replaced by serine in each peptide. Peptides were prepared as mixed disulfides with mercaptoethanol.

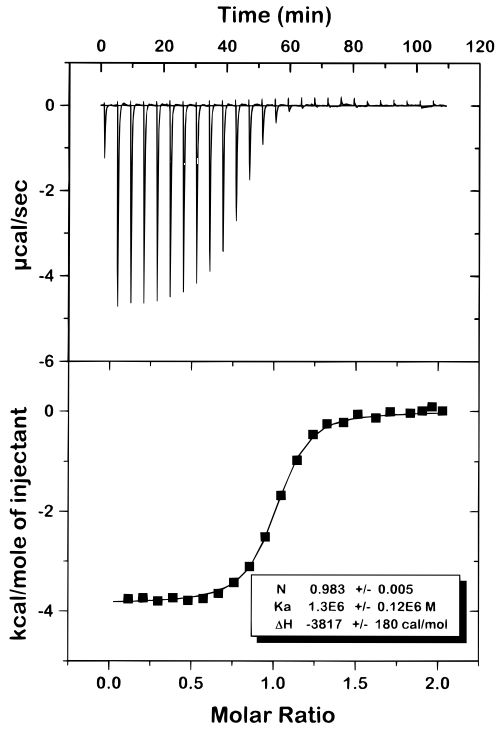

FIGURE 2: Isothermal calorimetric titration of GrxC14S with the oxidized C-terminal B1 25-mer peptide. (Top) Raw data from the addition of 10 μL aliquots of 1.0 mM oxidized peptide to a 0.15 mM solution of GrxC14S. (Bottom) Results from the least-squares fit to a one-binding site model of the heat exchanged per mole of peptide versus the molar ratio of peptide to protein.

Grx. Interestingly, both of the peptides display rapid rates of reaction with the protein, indicating that they are indeed good substrates for Grx. The longer peptide shows a larger overall oxidation of the protein, measured as the overall fluorescence change, that is closer to that obtained with GSSG, apparently indicating a more oxidizing redox potential for this peptide than the shorter one. On the basis of these results, we have focused our subsequent efforts on the 25-residue peptide. To provide additional confirmation of a substantial binding interaction between Grx and this C-terminal peptide, we have carried out calorimetric measurements on the binding of GrxC14S with the disulfide form of the 25-mer peptide. Figure 2 shows the results of these measurements which establish a 1:1 stoichiometry for binding of the peptide to the protein and establish a K_d for this process of 0.75 μM. Similar measurements of the binding of oxidized glutathione yield a K_d for that process of 1.5 μM (data not shown); thus, the peptide binds with an affinity very similar to that observed for glutathione. Measurements of the K_m of glutaredoxin for ribonucleotide reductase yield a value of 0.15 μM (*42*). Although a comparison of these values must be made with caution, the similarity of the measured K_d for the peptide and the K_m measured with ribonucleotide reductase suggests that the majority of the binding determinants reside in this region of the polypeptide chain.

Determination of the Electrophilic Cysteine in the 25-mer Peptide. To prepare a physiologically relevant mixed disulfide intermediate between Grx and the B1 peptide for structural studies, we must first determine which of the two cysteines in the peptide is the site of attack for the nucleophilic thiol of Grx. Additionally, this determination sheds light on the order of events associated with the reduction of the B1 subunit and the transfer of those reducing equivalents to the inner-pair active site disulfide. To determine this, we have again employed the fluorescence assay utilizing mutant 15-mer peptides in which one or the other of the cysteines has been replaced by serine and the remaining cysteine has been oxidized with HED to provide a mixed disulfide substrate for Grx. Shown in Figure 1B are the results of these assays. Replacement of the more C-terminal of the two cysteines with a serine results in a peptide that reacts relatively slowly with the protein, whereas replacement of the N-terminal cysteine with serine results in a peptide that displays the rapid reactivity observed with the disulfide forms of the peptide. This clearly demonstrates that attack of the nucleophilic thiol of Grx occurs first at the C-terminal cysteine.

The selectivity observed may be understood on the basis of the electrostatic distribution in the peptide. The sequence of the 25-mer peptide from the B1 subunit of *E. coli* ribonucleotide reductase is shown in Figure 3 along with the corresponding C-terminal sequences from a number of other species (*43*−*48*). Examination of the sequence from *E. coli* shows a glutamate neighboring the N-terminal cysteine as well as two aspartic acids located one and two residues away giving a negatively charged local environment around this cysteine, whereas the C-terminal cysteine has a neighboring lysine residue giving a positive local electrostatic environment. As the nucleophilic thiol of Grx is known to have a low pK_a of 4.5 (*49*), it exists in solution as a thiolate anion and is therefore negatively charged. This anion will be attracted to the positively charged environment surrounding the C-terminal cysteine and repelled from the negatively charged environment surrounding the N-terminal cysteine, thus providing the observed selectivity. Interestingly, examination of the C-terminal sequences of the B1 subunit of ribonucleotides reductases from a number of other species (Figure 3) consistently shows negatively charged residues in the vicinity of the more N-terminal of the two cysteines, indicating that this electrostatic-based discrimination probably plays a role in this interaction in those species as well.

Preparation of a Mixed Disulfide between GrxC14S and Ribonucleotide Reductase B1 (736−*761) (C754S).* The mixed disulfide between GrxC14S and B1 (736−761) (C754S) was prepared by treatment of the reduced mutant protein with a slight excess of the peptide which was prepared as a mixed disulfide with mercaptoethanol. Isoelectric focusing gel electrophoresis of the resulting complex gave a single band that displayed a considerably more acidic p*I* than the protein itself, in agreement with the attachment of the highly acidic peptide (overall charge of −6). Additionally, comparison of reverse-phase HPLC analysis of the complex itself and the complex in the presence of the reducing agent DTT showed one species for the complex which could be reduced by DTT to give two species, corresponding to the peptide and the protein. To facilitate NMR analysis of the complex, the protein was initially labeled with ^{15}N and ^{15}N half-filtered (*50*) COSY, NOESY, and ROESY spectra were recorded. Despite the modest size of the peptide, there was substantial overlap in these two-dimensional spectra that suggested the complete analysis would be difficult. To overcome these difficulties, we have

																		754					759		
															*	*		*	*	*	*	*	*	*	*
E. COLI	G	A	E	D	A	Q	D	D	L	V	P	S	I	Q	D	D	G	C	E	S	G	A	C	K	I
SALMONELLA	Y	Y	I	R	L	R	Q	L	A	L	E	G	T	E	I	E	G	C	V	S	-	-	C	A	L
MYCOPLASMA	R	Q	D	V	L	K	D	S	E	D	H	T	I	K	I	K	D	C	E	V	-	-	C	S	I
VACCINIA V.	K	D	K	I	K	P	P	V	V	C	D	S	-	-	-	E	I	C	T	S	-	-	C	S	G
VACCINIA C.	K	D	K	I	K	P	L	V	V	C	D	S	-	-	-	E	I	C	T	S	-	-	C	S	G
YEAST	D	I	Y	N	S	K	V	I	A	C	A	I	D	N	P	E	A	C	E	M	-	-	C	S	G
MOUSE	K	E	R	N	T	A	A	M	V	C	S	L	E	N	R	E	E	C	L	M	-	-	C	G	S
HUMAN	K	E	R	N	T	A	A	M	V	C	S	L	E	N	R	D	E	C	L	M	-	-	C	G	S

FIGURE 3: Alignment of the C-terminal sequences of the B1 subunit of ribonucleotide reductase from several species. Solid boxes show negatively charged amino acids close to the less reactive Cys 754 for *E. coli*. Residues showing intermolecular NOEs (*) are indicated on the *E. coli* sequence.

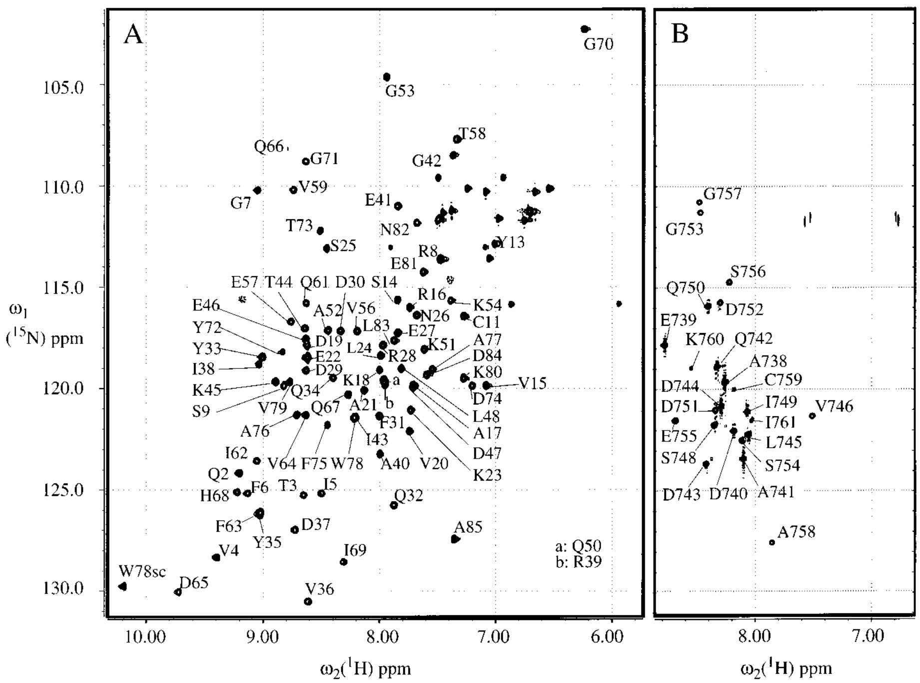

FIGURE 4: Panels A and B show the ^{15}N$-^1$H HSQC spectra of selectively labeled [^{15}N]Grx$-$B1 and Grx$-$[^{15}N]B1 complexes, respectively.

also prepared ^{15}N-labeled peptide via a biosynthetic strategy for the synthesis of the peptide developed by Walsh and co-workers (*35*). This strategy has allowed us to obtain uniformly ^{15}N-labeled peptide which was attached to unlabeled protein. Figure 4 shows ^{15}N$-^1$H HSQC spectra of the ^{15}N-labeled protein and peptide in the corresponding complexes. The HSQC spectrum of the peptide displays a number of additional peaks corresponding to a minor conformer of the peptide. Full assignment of the resonances of the peptide has shown that the second conformer results from a mixture of cis and trans proline at position 746. Such mixtures of cis and trans proline are commonly observed in flexible peptides (*51*). Both $\alpha-\alpha$ and $\alpha-\delta$ NOEs are observed from the proline to the preceding valine which is consistent with a mixture of cis and trans proline at this position. Additionally, all the doubled residues are located close to the proline, in agreement with cis$-$trans isomerism at this position being the source of this minor conformer.

To accelerate the assignment process as well as to enable the use of both ^{13}C and ^{15}N half-filter techniques that will provide unequivocal assignment of protein$-$peptide NOEs, complexes of fully ^{15}N- and ^{13}C-labeled peptide and protein have been prepared and coupled to unlabeled protein or peptide as appropriate. Table 1 shows the experiments that have been recorded on the protein and the peptide to obtain complete heteronuclear backbone and side chain assignments. The assignments for the peptide and protein are available as Supporting Information.

Mapping of the Peptide Binding Site on Glutaredoxin. Figure 5 shows strips from three-dimensional (3D) ^{13}C- and ^{15}N-edited NOESY spectra recorded with the ^{13}C and ^{15}N half-filter element of Hallenga and co-workers (*52*) appended to the indirect proton dimension. In the manner in which these spectra were recorded, intra- and intermolecular NOEs have a 180° phase difference with respect to one another, providing an unequivocal identification of inter- versus intramolecular NOEs. On the basis of these NOESY data, we have mapped the binding site for the peptide onto the known structure of reduced *E. coli* Grx as shown in Figure 6. All the NOEs between the peptide and protein displayed in Figure 6 have been confirmed by observation in spectra of labeled peptide and of labeled protein to eliminate possible misinterpretation based on intramolecular NOEs to unabeled protons such as the hydroxyls of Thr, Ser, and Tyr. An extensive interaction surface is observed which includes the active site, the previously identified glutathione binding site (*21*), residues on one face of α-helix 1, the loop connecting

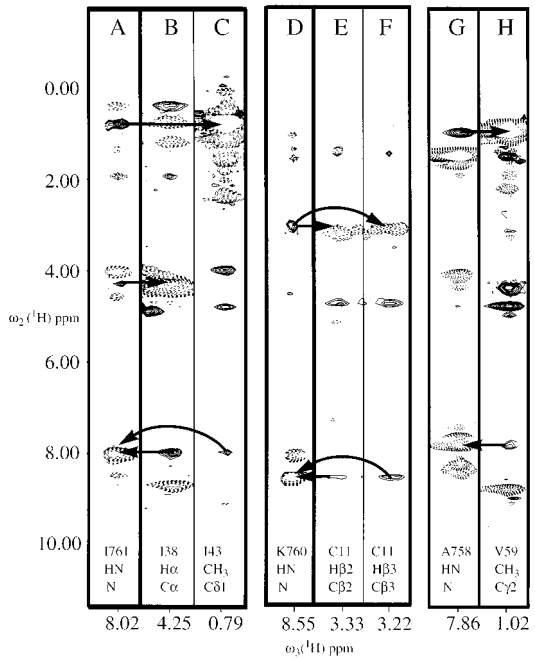

FIGURE 5: Strips from the 3D ^{15}N-edited NOESY spectrum of the Grx−[^{15}N,^{13}C]B1 complex (panels A, D, and G) and from the 3D ^{13}C-edited NOESY spectrum of the [^{15}N,^{13}C]Grx−B1 complex (panels B, C, E, F, and H), both recorded with the half-filter element of Hallenga and co-workers (*52*) appended to the indirect ^{1}H dimension. Dashed contour lines represent intramolecular NOEs, and solid contour lines represent intermolecular NOEs. Arrows indicate several intermolecular NOEs that have been confirmed in both spectra.

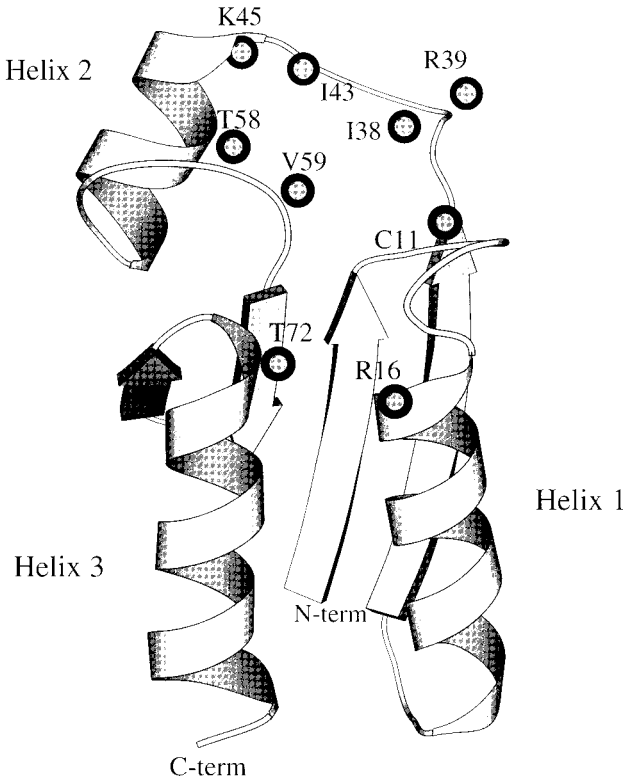

FIGURE 6: Identification of residues showing intermolecular NOEs to the peptide mapped onto a schematic ribbon representation of the structure of reduced glutaredoxin created using MOLSCRIPT (*64*).

β-strand 2 to α-helix 2, and the N-terminal region of α-helix 2. The structure of the mixed disulfide between GrxC14S and glutathione showed the glutathione to be in an antiparallel orientation with respect to the short extended element running from V56 to V59 with the Gly extending toward α-helix 2. Assuming the peptide adopts a similar orientation for its C-terminal end, contacts with the loop connecting β-strand 2 to α-helix 2 and the N-terminal region of α-helix 2 could result from the presence of two residues C-terminal to the Cys in the peptide versus only one in GSH allowing the peptide to make contacts with residues in this region of the protein.

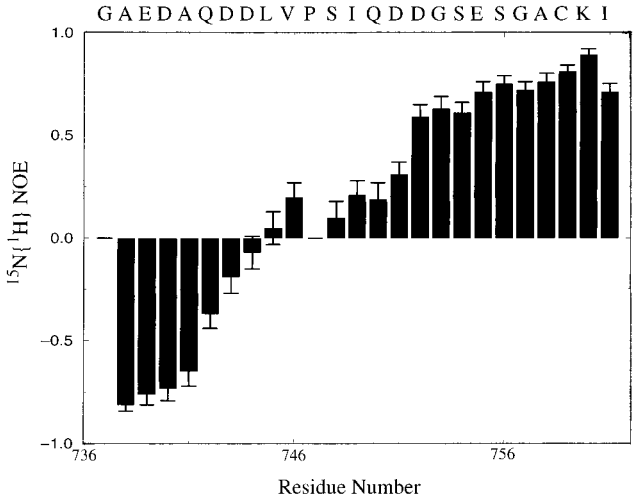

FIGURE 7: Plot of the {^{1}H}−^{15}N NOE as a function of residue number for the backbone ^{15}N nuclei of the Grx−[^{15}N]B1 mixed disulfide.

Mapping of the Peptide Binding Regions. To obtain preliminary evidence identifying residues of the peptide that are bound tightly to the protein, we have identified those residues in the peptide that are displaying intermolecular NOEs to the protein in the ^{13}C and ^{15}N-half-filtered 3D ^{13}C- and ^{15}N-edited NOESY spectra recorded on a sample of doubly labeled peptide attached to unlabeled protein. As shown in Figure 3, the 11 C-terminal residues of the peptide are showing intermolecular NOEs to the protein, indicating intimate contact between this portion of the peptide and the protein. We have also determined the backbone {^{1}H}−^{15}N NOE values for the bound ^{15}N-labeled peptide to characterize the dynamics of the peptide in the bound form. As seen in Figure 7, the 10 C-terminal residues have values for the {^{1}H}−^{15}N NOE quite similar to those observed for the nonmobile portion of glutaredoxin-1 (*53*). The values observed for the 10 C-terminal residues indicate that this region of the peptide is tightly bound to the protein. Continuing toward the N terminus of the peptide, there are six residues following the 10 C-terminal residues that still display positive values for the {^{1}H}−^{15}N NOE, indicating some degree of rigidity, whereas the final seven residues display negative values for the {^{1}H}−^{15}N NOE, indicative of a high degree of mobility. Interestingly, the above-mentioned fluorescence assays showed the longer 25-mer peptide to be a more effective oxidant of Grx than the shorter 15-mer peptide. As the N-terminal residues are unlikely to perturb the environment around the peptide disulfide due to their flexibility and their distance from the cysteine residues, it appears that this difference in redox potential arises from an increased affinity for the protein. Four of the residues in this more mobile N-terminal portion of the peptide are

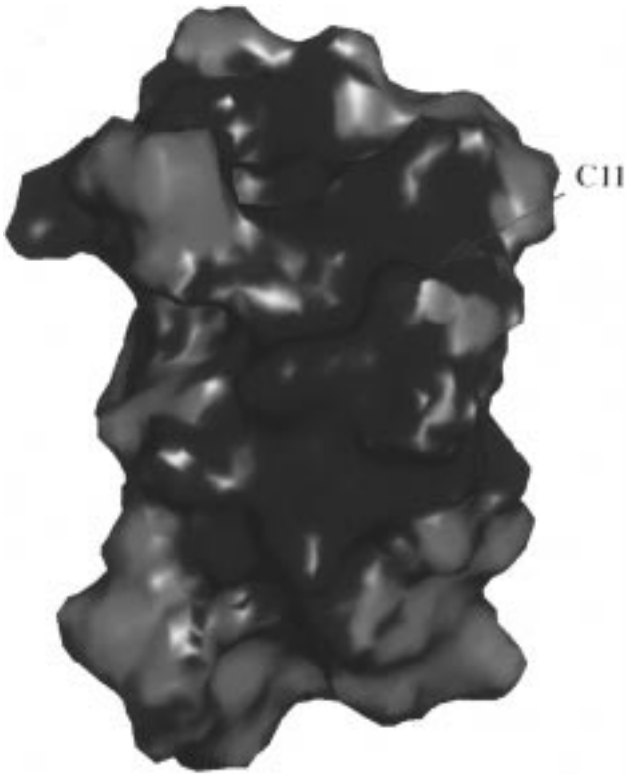

FIGURE 8: Electrostatic potential distribution, mapped on a surface defined by the reduced form of Grx. The protein orientation is equivalent to the one shown in Figure 6. Blue and red areas are associated with regions of positive and negative charge, respectively.

negatively charged, suggesting that the electrostatic field associated with these residues plays a role in the binding to the protein. The electrostatic potential of the surface of Grx surrounding the active site suggests this may be the case (see below). Chemical shift index (CSI) analysis (*65*) of the backbone chemical shifts and analysis of the sequential NOEs has been carried out to determine if the peptide adopts any type of regular secondary structure in the bound form. Consensus CSI analysis yields coil values for the entire length of the peptide. At the more well defined C-terminal end of the peptide, residues 754−758 do yield CB chemical shifts indicative of a β conformation. This is consistent with the sequential NOEs observed in that we observe strong $d_{\alpha N}$ but not d_{NN} sequential NOEs for the 11 protein-bound C-terminal residues. Thus, the bound portion of the peptide appears to adopt an extended secondary structure but cannot be characterized as a regular β conformation.

Role of Electrostatics in Binding of Grx to Ribonucleotide Reductase B1. Figure 8 shows the electrostatic potential surface of reduced glutaredoxin, with positively charged regions in blue and negatively charged regions in red. There is a substantial positive patch located in the vicinity of the active site. The electrostatic potential has been calculated with a thiolate for Cys 11 on the basis of the pK_a of 4.5 observed for this thiol. The thiolate of Cys 11 is located in the boundaries of this positively charged patch. A similar calculation that uses a thiol group (SH) instead of the thiolate (S^-) for Cys 11 extends the positive patch over Cys 11, which may help to explain its surprisingly low pK_a by favoring the formation of the thiolate. Inclusion of this Cys residue as a thiolate diminishes somewhat the extent of the positive potential in the vicinity of the active site, but a substantial positive potential remains. As the peptide is highly negatively charged, this attractive potential in the vicinity of the active site is likely to play an important role in its binding to the B1 peptide. In addition, Figure 9 shows the dipole moment arising from the particular orientation of the charge separation produced by the protein structure. This dipole moment is seen to extend directly from the active site which will increase the likelihood of a productive binding interaction by guiding the highly negatively charged peptide into the active site, thereby enhancing the on rate for binding and thus the overall equilibrium binding constant.

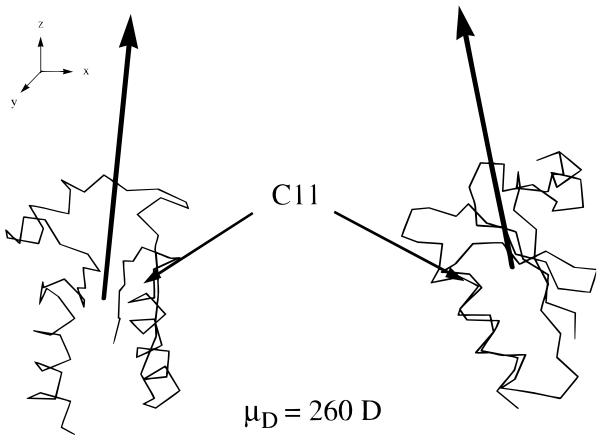

FIGURE 9: Molecular dipole moment for reduced Grx. The orientation of the dipole moment vector is indicated in two views (rotated by −90° along *z*) of a Cα trace representation of the protein.

CONCLUSIONS

We have prepared and characterized a specific complex between *E. coli* glutaredoxin-1 (C14S) and a peptide derived form the C-terminus of the B1 subunit of ribonucleotide reductase. We have shown the 10 C-terminal residues of the peptide appear to be bound tightly to the protein, whereas the remainder of the peptide does not appear to be tightly bound; however, these N-terminal residues contribute to the overall binding probably through electrostatic interactions. The bound portion of the peptide seems to adopt an extended conformation, but no regular secondary structure could be identified for this region of the peptide. The binding site for the peptide has been mapped on glutaredoxin and shown to span a relatively large area, including the active site and GSH binding site. The electrostatic potential of the protein in the vicinity of the active site provides an excellent match for the binding of the highly negatively charged B1 peptide; thus, electrostatic interactions appear to be an important component of the interaction between Grx and the B1 subunit of ribonucleotide reductase. Complete heteronuclear NMR resonance assignments of the protein and the peptide as well as NOE information have been obtained, and the determination of the 3D structure of this important complex is underway.

ACKNOWLEDGMENT

We thank Dr. Nancy Speck and Mr. Ting-Lei Gu for their advice in the cloning of the peptide coding DNA. We also thank Mr. Wayne Casey for his help in maintaining our NMR spectrometer.

SUPPORTING INFORMATION AVAILABLE

^{1}H, ^{13}C, and ^{15}N assignments for the 85 residues corresponding to GrxC14S and the ^{1}H, ^{13}C, and ^{15}N assignments for residues 737−761 of the B1 peptide, both in the mixed disulfide (7 pages). Ordering information is given on any current masthead page.

REFERENCES

1. Ahn, B., and Moss, B. (1992) *Proc. Natl. Acad. Sci. U.S.A. 89* 7060−7064.
2. Gan, Z.-R., and Wells, W. W. (1987) *J. Biol. Chem. 262*, 6699−6703.
3. Gan, Z.-R., Polokoff, M. A., Jacobs, J. W., and Sordana, M. K. (1990) *Biochem. Biophys. Res. Commun. 168*, 944−951.
4. Höög, J.-O., Jörnvall, H., Holmgren, A., Carlquist, M., and Persson, M. (1983) *Eur. J. Biochem. 136*, 223−232.
5. Hopper, S., Johnson, R. S., and Biemann, K. (1989) *J. Biol. Chem. 264*, 20438−20447.
6. Johnson, G. P., Goebel, S. J., Perkus, M. E., Davis, S. W., Winslow, J. P., and Paoletti, E. (1991) *Virology 181*, 378−381.
7. Klintrot, I.-M., Höög, J.-O., Jörnvall, H., Holmgren, A., and Luthman, M. (1984) *Eur. J. Biochem. 144*, 417−423.
8. Minakuchi, K., Yabushita, T., Masumura, T., Ichihara, K., and Tanaka, K. (1994) *FEBS Lett. 337*, 157−160.
9. Padilla, C. A., Martínez-Galisteo, E., Bárcena, J. A., Spyrou, G., and Holmgren, A. (1995) *Eur. J. Biochem. 227*, 27−34.
10. Åslund, F., Nordstrand, K., Berndt, K. D., Nikkola, M., Bergman, T., Ponstingl, H., Jörnvall, H., Otting, G., and Holmgren, A. (1996) *J. Biol. Chem. 271*, 6736−6745.
11. Holmgren, A. (1976) *Proc. Natl. Acad. Sci. U.S.A. 73*, 2275−2279.
12. Holmgren, A. (1979) *J. Biol. Chem. 254*, 3664−3671.
13. Luthman, M., Eriksson, S., Holmgren, A., and Thelander, L. (1979) *Proc. Natl. Acad. Sci. U.S.A. 76*, 2158−2162.
14. Luthman, M., and Holmgren, A. (1982) *J. Biol. Chem. 257*, 6686−6690.
15. Russel, M., Model, P., and Holmgren, A. (1990) *J. Bacteriol. 172*, 1923−1929.
16. Tsang, M. L. (1981) *J. Bacteriol. 146*, 1059−1066.
17. Gladysheva, T. B., Oden, K. L., and Rosen, B. P. (1994) *Biochemistry 33*, 7288−7293.
18. Wells, W. W., Peng Xu, D., Yang, Y., and Rocque, P. A. (1990) *J. Biol. Chem. 265*, 15361−15364.
19. Gravina, S., and Mieyal, J. (1993) *Biochemistry 32*, 3368−3376.
20. Jung, C., and Thomas, J. (1996) *Arch. Biochem. Biophys. 335*, 1, 61−72.
21. Bushweller, J., Billeter, M., Holmgren, A., and Wüthrich, K. (1994) *J. Mol. Biol. 235*, 1585−1597.
22. Gilbert, H. F. (1990) *Adv. Enzymol. Relat. Areas Mol. Biol. 63*, 69−172.
23. Thomas, J. A., Poland, B., and Honzatko, R. (1995) *Arch. Biochem. Biophys. 319*, 1−9.
24. Martin, J. L. (1995) *Structure 3*, 245−250.
25. Kren, B., Parsel, D., and Fuchs, J. (1988) *J. Bacteriol. 170*, 308−315.
26. Stubbe, J. (1990) *Adv. Enzymol. Relat. Areas Mol. Biol. 63*, 349−419.
27. Sjöberg, B. M., Graslund, A., and Eckstein, F. (1983) *J. Biol. Chem. 258*, 8060−8067.
28. Mao, S. S., Holler, T. P., Yu, G. X., Bollinger, J. M., Jr., Booker, S., Johnston, M. I., and Stubbe, J. (1992) *Biochemistry 31*, 9733−9743.
29. Åberg, A., Hahne, S., Karlsson, M., Larsson, A., Ormö, M., Ahgren, A., and Sjöberg, N. M. (1989) *J. Biol. Chem. 264*, 12249−12252.
30. Mao, S. S., Yu, G. X., Chalfuoun, D., and Stubbe, J. (1992) *Biochemistry 31*, 9752−9759.
31. Uhlin, U., and Eklund, H. (1994) *Nature 370*, 533−539.
32. Qin, J., Clore, M., Poindexter Kennedy, W., Huth, J. R., and Gronenborn, A. (1995) *Structure 3*, 289−297.
33. Qin, J., Clore, M., Poindexter Kennedy, W. M., and Gronenborn, A. (1996) *Structure 4*, 613−620.
34. Björnberg, O., and Holmgren, A. (1991) *Protein Expression Purif. 2*, 287−295.
35. Kuliopulos, A., and Walsh, C. (1994) *J. Am. Chem. Soc. 116*, 4599−4607.
36. Sambrook, J., Fritsch, E. F., and Maniatis, T. (1989) *Molecular Cloning: A Laboratory Manual*, 2nd ed., Cold Spring Harbor Laboratory Press, Cold Spring Harbor, NY.
37. Güntert, P., Dötsch, V., Wider, G., and Wüthrich, K. (1992) *J. Biomol. NMR 2*, 619−629.
38. Bartels, C., Xia, T., Billeter, M., Güntert, P., and Wüthrich, K. (1995) *J. Biomol. NMR 6*, 1−10.
39. Sodano, P., Xia, T., Bushweller, J. H., Björnberg, O., Holmgren, A., Billeter, M., and Wüthrich, K. (1991) *J. Mol. Biol. 221*, 1311−1324.
40. Bushweller, J. H., Åslund, F., Wüthrich, K., and Holmgren, A. (1992) *Biochemistry 31*, 9288−9293.
41. Björnberg, O., and Holmgren, A. (1993) Private communication.
42. Holmgren, A. (1979) *J. Biol. Chem. 254*, 9113−9119.
43. Parker, N., Begley, C., and Fox, R. (1991) *Nucleic Acids Res. 19*, 3741−3741.
44. Tengelsen, I., Slabaugh, M., Bibler, J. K., and Hruby, D. (1988) *Virology 164*, 121−131.
45. Goebel, S., Johnson, G., Perkus, M., Davis, S., Winslow, J., and Paoletti, E. (1990) *Virology 179*, 247−266.
46. Nilsson, O., Anders, A., Tomas, L., and Sjoeberg, B. (1988) *Nucleic Acids Res. 16*, 4174.
47. Jordan, A., Gibert, I., and Barbe, J. (1994) *J. Bacteriol. 176*, 3420−3427.
48. Caras, I., Levinson, B., Fabry, M., Williams, R., and Martin, D., Jr. (1985) *J. Biol. Chem. 260*, 7015−7022.
49. Kallis, G. B., and Holmgren, A. (1980) *J. Biol. Chem. 255*, 10261−10265.
50. Otting, G., and Wüthrich, K. (1988) *J. Magn. Reson. 76*, 569−574.
51. Wüthrich, K. (1976) *NMR in Biological Research: Peptides and Proteins*, North Holland, Amsterdam.
52. Folmer, R., Hilbers, C., Konings, R., and Hallenga, K. (1995) *J. Biomol. NMR 5*, 427−432.
53. Kelley, J., Caputo, T., Eaton, S., Laue, T., and Bushweller, J. (1997) *Biochemistry 36*, 5029−5044.
54. Kay, L. E., Keifer, P., and Saarinern, T. (1992) *J. Am. Chem. Soc. 114*, 10663−10665.
55. Zhang, O., Kay, L. E., Olivier, J. P., and Forman-Kay, J. D. (1994) *J. Biol. NMR 4*, 845−858.
56. Bax, A., and Davies, D. (1985) *J. Magn. Reson. 63*, 207−213.
57. Muhandiram, D. R., and Kay, L. E. (1994) *J. Magn. Reson., Ser. B 103*, 203−216.
58. Tashiro, M., Rios, C., and Montelione, G. (1995) *J. Biomol. NMR 6*, 211−216.
59. Kay, L. E., Xu, G., Singer, A. U., Muhandiram, D. R., and Forman-Kay, J. D. (1993) *J. Magn. Reson., Ser. B 101*, 333−337.
60. Vuister, G. W., and Bax, A. (1992) *J. Magn. Reson. 98*, 428−435.
61. Yamazaki, T., Forman-Kay, J. D., and Kay, L. E. (1993) *J. Am. Chem. Soc. 115*, 11054−11055.
62. Live, D. H., Davis, D. G., Agosta, W. C., and Cowburn, D. (1984) *J. Am. Chem. Soc. 106*, 1939−1941.
63. Bax, A., and Subramanian, S. (1986) *J. Magn. Reson. 67*, 565−569.
64. Kraulis, P. J. (1991) *J. Appl. Crystallogr. 24*, 946−950.
65. Wishart, D. S., and Sykes, B. D. (1994) *J. Biomol. NMR 4*, 171−180.

BI972924D